Current Biology 23, 196–203, February 4, 2013 ©2013 Elsevier Ltd All rights reserved http://dx.doi.org/10.1016/j.cub.2012.12.024

Article

A Novel Actin-Binding Motif in Las17/WASP Nucleates Actin Filaments Independently of Arp2/3

Agnieszka N. Urbanek,[1,2] Adam P. Smith,[1,2] Ellen G. Allwood,[1,2] Wesley I. Booth,[1] and Kathryn R. Ayscough[1,*]

[1]Department of Biomedical Science, Firth Court, University of Sheffield, Sheffield S10 2TN, UK

Summary

Background: Actin nucleation is the key rate-limiting step in actin polymerization, and tight regulation of this process is critical to ensure that actin filaments form only at specific regions of the cell. Las17 is the primary activator of Arp2/3-driven actin nucleation in yeast and is required for membrane invagination during endocytosis. Its mammalian homolog, WASP, has also been studied extensively as an activator of Arp2/3-driven actin polymerization. In both Las17 and WASP, actin nucleation activity is attributed to an ability to bind actin through a WH2 domain and to bind Arp2/3 through an acidic region. The central region of both Las17 and WASP is rich in proline residues and is generally considered to bind to SH3-domain-containing proteins.

Results: We have identified a novel actin-binding activity in the polyproline domain of both yeast Las17 and mammalian WASP. The polyproline domain of Las17 is also able to nucleate actin filaments independently of Arp2/3. Mutational analysis reveals that proline residues are required for this nucleation activity and that the binding site on actin maps to a region distinct from those used by other nucleation activities. In vivo analysis of yeast strains expressing *las17* mutated in the WH2 domain, one of its proline motifs, or both shows additive defects in actin organization and endocytosis, with the proline mutant conferring more severe phenotypes than the WH2 mutant.

Conclusions: Our data demonstrate a new actin-binding and nucleation mechanism in Las17/WASP that is required for its function in actin regulation during endocytosis.

Introduction

Actin is one of the most highly conserved and abundant eukaryotic proteins, playing a critical role in many cell processes ranging from motility, cell organization, and morphology to membrane trafficking. Actin monomers (G-actin) are assembled into dynamic polarized filaments (F-actin) that are regulated by an array of actin-associated proteins [1]. These proteins ensure that actin is assembled and disassembled at defined sites in response to specific internal and external cell signals. Although many stages of actin turnover are under regulation, the key rate-limiting step is that of actin nucleation, which can be defined as the formation of a stable multimer. Tight regulation of actin nucleation is necessary to ensure that filaments form only at specific regions of the cell [2].

Until recently, two major actin nucleators were recognized, the Arp2/3 complex and formins [2–5]. Arp2/3 is proposed to polymerize new filaments on the side of existing filaments. It is a weak nucleator alone and functions with nucleation-promoting factors such as WASP to form a branched actin network [6]. Formins function as dimers to assemble unbranched filaments. A recently described third group of nucleators, including Spire, Cordon-bleu, and Leiomodin, have a general mechanism of tandem actin monomer binding [5, 7]. All of these proteins contain one or more copies of the recognized actin-binding domain WH2, but also other domains that contribute further actin-binding function [8–10]. This increasingly recognized variation indicates there may be other nucleators with distinct architecture that have yet to be identified.

Las17, the homolog of WASP, is considered the primary nucleation-promoting factor for Arp2/3 in yeast [11, 12]. Similar to WASP, Las17 has a C-terminal WCA domain comprising a *W*H2 domain that binds monomeric actin and a *c*entral plus *a*cidic (CA) region that binds Arp2/3 [12]. Both Las17 and Arp2/3 localize to cortical actin patches, and they play a key role in driving the actin polymerization required for the formation of endocytic invaginations. Intriguingly, however, deletion of either the acidic region alone or the entire WCA domain of Las17 yields a very mild cellular phenotype, and actin organization at cortical patches appears normal [13, 14]. A further enigma in the function of Las17 is that it arrives at endocytic sites 10–15 s before Arp2/3, raising the possibility of an Arp2/3-independent function. Finally, Arp2/3 is generally considered to nucleate filaments on existing filaments [5]. The identity of the proteins capable of generating these initial filaments has not previously been addressed. Here we present data investigating a novel actin-binding function of Las17 that resides in its polyproline (PP) region.

Results

The Las17 Polyproline Fragment Binds Actin in Yeast Two-Hybrid Assays

Although Arp2/3 is activated by binding the Las17 WCA domain, polymerization assays have shown that inclusion of full-length Las17 gives higher levels of actin nucleation [15]. Furthermore, inclusion of the polyproline region with the WCA domain of WASP and SCAR in similar Arp2/3-driven assays also causes a significant increase in polymerization rate [16]. The nature of this additional contribution to actin polymerization kinetics has not been addressed. We aimed to determine whether the polyproline region of Las17 harbors further actin-interacting activity that might explain previous in vivo and in vitro findings.

Making use of an actin yeast two-hybrid construct successfully used in other studies to identify novel actin-binding proteins [17], we determined whether a full-length Las17 construct or a construct comprising its polyproline region (Las17PP) was able to interact with actin. The domains of Las17 used are illustrated in Figure 1A. As shown, β-galactosidase reporter assays reveal an interaction between Las17PP (amino acids 292–536) and actin (Figure 1B). Deletions from

[2]These authors contributed equally to this work
*Correspondence: k.ayscough@sheffield.ac.uk

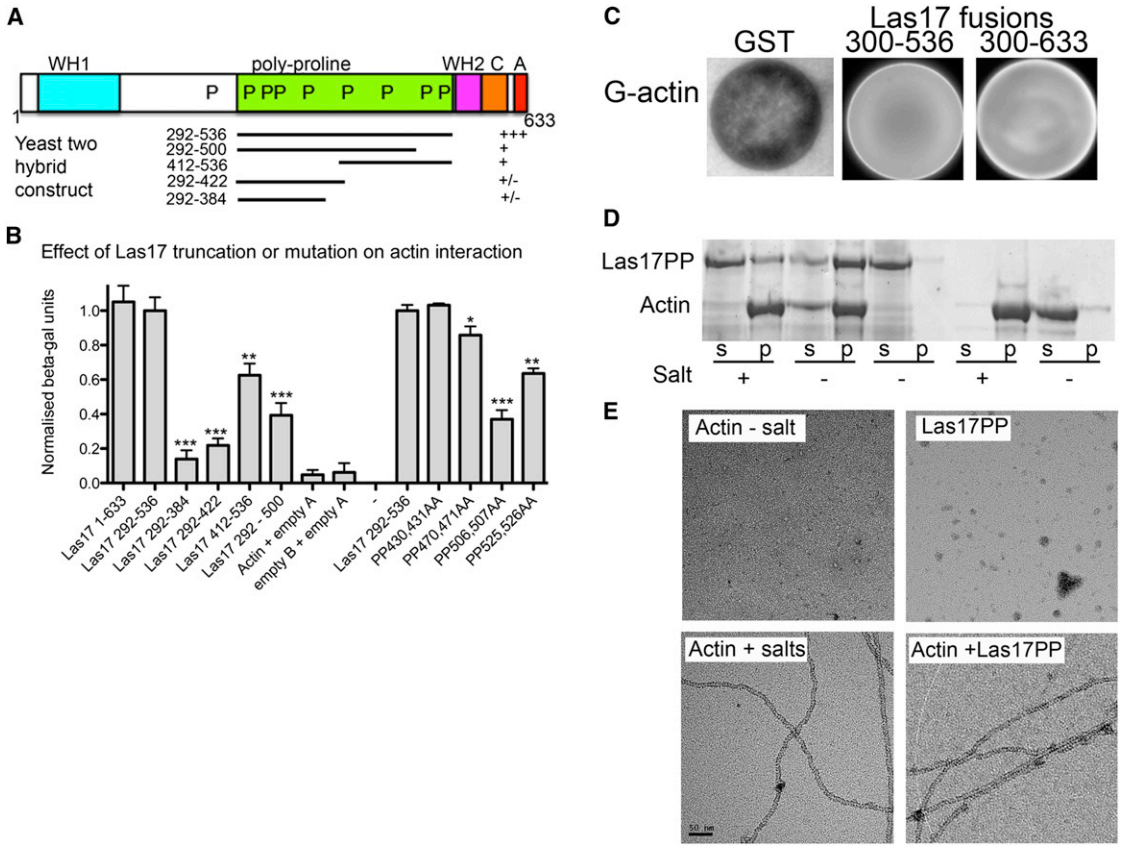

Figure 1. Las17 Interactions with Actin

(A) The domain structure of Las17 comprises an N-terminal WASP homology 1 region (WH1), central polyproline region (PP), WASP homology 2 region (WH2) that interacts with G-actin, and central and acidic regions (CA) that interact with Arp2/3. Positions of nine 5×PP tracts are marked P. A summary of yeast two-hybrid interactions from plate- and liquid-based assays for various truncations is below. The number of plus signs (+) indicates strength of interaction based on these approaches.

(B) Plasmids expressing Las17 truncation or PP mutations were transformed into pJ69-4 a and α strains and crossed. Strains were grown in liquid media, and β-galactosidase was assayed. Errors are SD for four or more independent assays. Results are normalized to data for Las17 292–536. Significance of changes versus Las17 292–536 by unpaired Student's two-tailed t test: ***$p < 0.0001$ for 292–384, 292–422, 292–500, and PP506,507AA mutants; **$p = 0.0003$ for 412–536; *$p = 0.0154$ for PP470,471AA; **$p = 0.0006$ for PP525,526AA.

(C) GST or GST-Las17 fragments were expressed and bound to glutathione beads and then incubated with G-actin in G buffer. Alexa 568 actin was added to samples to allow visualization of actin.

(D) Actin was polymerized in the presence or absence of salts including 50 mM KCl and/or in the presence of recombinant GST-Las17PP. Samples were spun to pellet F-actin and any associated proteins.

(E) Electron microscopy was performed to determine whether filaments were formed in the presence of Las17PP (GST cleaved).

both N and C termini of Las17PP reduced activation of the reporters, indicating either that multiple binding sites exist or that a single binding site is formed from residues at both ends of the construct. However, about 50% of reporter activity was lost on deletion of the final 36 amino acids. This was unexpected because there is no homology with known actin-binding proteins in this region.

Las17 has nine tracts of five proline residues (5×PP) (see Figure S1A available online), with eight of these in the region studied. Four 5×PP are also recognized SH3-binding motifs and contain adjacent basic residues that are proposed to contribute to SH3-domain binding, whereas the C-terminal 5×PP tracts do not have associated basic residues and have not been identified as SH3-binding sites [18]. Within the 36 aa region (aa 500–536) that makes the most significant contribution to actin binding in the yeast two-hybrid assay are two 5×PP stretches, suggesting a possible proline-based actin-binding motif. To test this, prolines in the most C-terminal four tracts were mutagenized. As shown in Figure 1B, mutagenesis of three of these sites reduced the interaction, indicating a contribution by prolines to actin binding, with more C-terminal tracts playing a predominant role.

Las17 Binds Directly to Actin and Drives Polymerization In Vitro

It is well documented that profilin can bind to polyproline regions in actin-binding proteins, and it is proposed to aid delivery of actin monomers for polymerization [19, 20]. However, direct binding of profilin to Las17 has not been reported. In addition, although verprolin binds both Las17 and profilin, the Las17-verprolin interacting region is not part of the Las17 region used in the yeast two-hybrid assays [21]. This suggests that Las17PP may interact directly with actin. To test this, we generated glutathione S-transferase (GST) fusions of Las17PP and Las17PP+WCA on Sepharose beads and incubated them with actin containing a low level of fluorescently labeled actin

to detect binding. Although association of Las17PP+WCA with actin was predicted due to the presence of the well-characterized monomer-binding WH2 domain, similar binding of Las17PP alone was unexpected (Figure 1C). In contrast, GST alone on beads shows no association with actin.

A high-speed centrifugation assay is frequently used to demonstrate F-actin binding (Figure 1D). In the presence of salt, actin is induced to polymerize and enter the pellet fraction. GST-Las17PP when incubated with actin also shifts to the pellet, demonstrating binding. Unexpectedly, in the absence of salt, when actin alone is unable to pellet, addition of GST-Las17PP (but no salt) also causes pelleting, indicating that Las17PP binds actin and potentially nucleates its polymerization. In order to ascertain whether the actin was pelleting due to filament formation rather than simply aggregating, samples were analyzed by electron microscopy. Filaments formed in the presence of Las17PP (cleaved from GST) were very similar to those formed in the presence of salt (Figure 1E).

Las17PP Nucleates Actin Filaments

Absence of salt is nonphysiological, so to investigate the possibility of nucleation further, a pyrene-actin polymerization assay was performed in the presence of salts. Incorporation of pyrene-labeled actin into filaments as they form can be detected fluorometrically as an enhanced fluorescence signal. Actin (5 μM) was polymerized with increasing levels of Las17PP. Using this approach, measurements were made to determine the affinity of Las17 binding to actin, giving a K_d of 0.22 μM (Figure S2).This is comparable to the apparent affinity reported of 0.4 μM for WASP WCA domain with actin [22]. These assays also revealed that in the presence of Las17PP, the lag phase of polymerization is reduced, indicating that the PP region nucleates actin filaments in the absence of other proteins (Figure 2A). In addition, the rate of polymerization and the final level of F-actin at steady state are increased. These data demonstrate that Las17PP interacts with actin and can trigger both nucleation and increased polymerization. The higher final amount of polymerized actin observed at steady state suggests that the fragment is able to reduce the critical concentration of actin in the reaction.

If Las17PP nucleates actin filaments de novo, then an increased number of filaments should be generated in a given time. To test this, we determined the number of filaments formed after polymerization induction using fluorescence microscopy. Actin (3 μM + 0.4 μM Alexa 568-labeled actin) was induced to polymerize, samples were taken after 30 min, and the number of filaments per grid square was counted. As shown in Figures 2B and 2C, there was a significant increase in filament number following addition of Las17PP, further supporting the presence of nucleating activity.

Two questions were then addressed. First, does the number of PP tracts affect the ability to nucleate actin? Second, are prolines central to activity? A 28-mer peptide of Las17PP (residues 501–528) was synthesized and incubated with actin. The peptide did not substantially reduce the lag phase of actin polymerization, suggesting that the ability to nucleate is a function of having more than two 5×PP tracts (Figure 2D). However, peptide addition did cause an increased polymerization rate and final level of F-actin. Mutation of both PP tracts from PPPPP to PPPAA completely blocked the effect of the peptide on actin dynamics, demonstrating the critical role played by proline residues in the actin interaction.

A fragment carrying all eight 5×PP tracts but mutagenized at the site contributing most actin-binding activity in yeast two-hybrid analysis (PP506,507AA; Figure 1B) was also purified. This fragment nucleated actin, shown by a reduced lag phase, but overall F-actin level at steady state was reduced (Figure 2E). This supports the idea that multiple 5×PP interaction sites can promote actin nucleation and demonstrates that the PP506,507 site plays an important role in binding actin, potentially reducing the critical concentration during polymerization.

The Polyproline Region in WASP Interacts with Actin

To determine whether PP tracts in other related proteins are able to function in a manner similar to Las17PP, we subcloned the polyproline region of human WASP (amino acids 300–430) to generate a GST fusion. This region contains four tracts of five or more proline residues. After cleavage from GST, recombinant WASP-PP was incubated with actin in a pyrene assay (Figure 2F). Under these conditions, higher concentrations of WASP-PP increase the overall level of F-actin polymerized but do not cause a reduction in lag phase. Electron microscopy revealed actin filaments when G-actin was incubated with WASP-PP (Figure 2G).

Together, the in vitro data with purified proteins demonstrate that both Las17 and WASP-PP regions can interact with actin directly and thereby enhance actin polymerization. The interaction specifically requires prolines. If PP tracts contribute actin-binding function alone, or in concert with other domains, such tracts may function similarly in other actin-binding proteins, which might indicate additional functionality for such proteins. We performed a genome-wide search for proteins containing two or more tracts of five proline residues. Surprisingly, there are only eight such proteins in the *Saccharomyces cerevisiae* genome, and intriguingly, five of these proteins (formins Bni1 and Bnr1 and the Arp2/3 nucleation-promoting factors Las17, Vrp1, and Pan1) have been directly linked to actin nucleation. Of the remaining three proteins, Eap1 has been linked with TOR signaling and has been detected in a screen for genes involved in endocytosis [23, 24]. Analysis of all *S. cerevisiae* proteins with a single 5×PP is shown in Table S1 and Figure S3.

Mapping Binding of Las17PP to Actin

Given that both the WH2 domain and profilin are known to bind at the barbed end of an actin monomer [25, 26], it was of interest to determine whether the actin-binding site for Las17PP bound the same site or a distinct surface of actin. To map the binding site of Las17PP, we used a yeast two-hybrid approach in which a Gal4 binding domain (Gal4BD)-actin fusion was mutated to generate mutant actin alleles. This alanine-scan collection has been used to map interactions between actin and Aip1 [17]. An interaction between actin and Las17PP was assessed in strains carrying 27 actin alleles. In two cases, *act1-104* and *act1-111*, no growth was observed (Figure 3A), indicating that the interaction was disrupted. In these mutants, expression of Gal4BD fusion was verified by western blotting (data not shown). The position of alleles within actin was then considered. *act1-104* carries the mutations K315A and E316A, and *act1-111* carries the mutations D222A, E224A, and E226A. These sites reside on a surface between subdomain III and IV on the monomer (Figure 3B), strongly implicating this region in Las17PP binding. Within the actin filament (Figure 3C), residues in each allele are exposed and available for interactions; thus, unlike WH2, which binds actin monomers, these sites can mediate binding to both G-actin and F-actin.

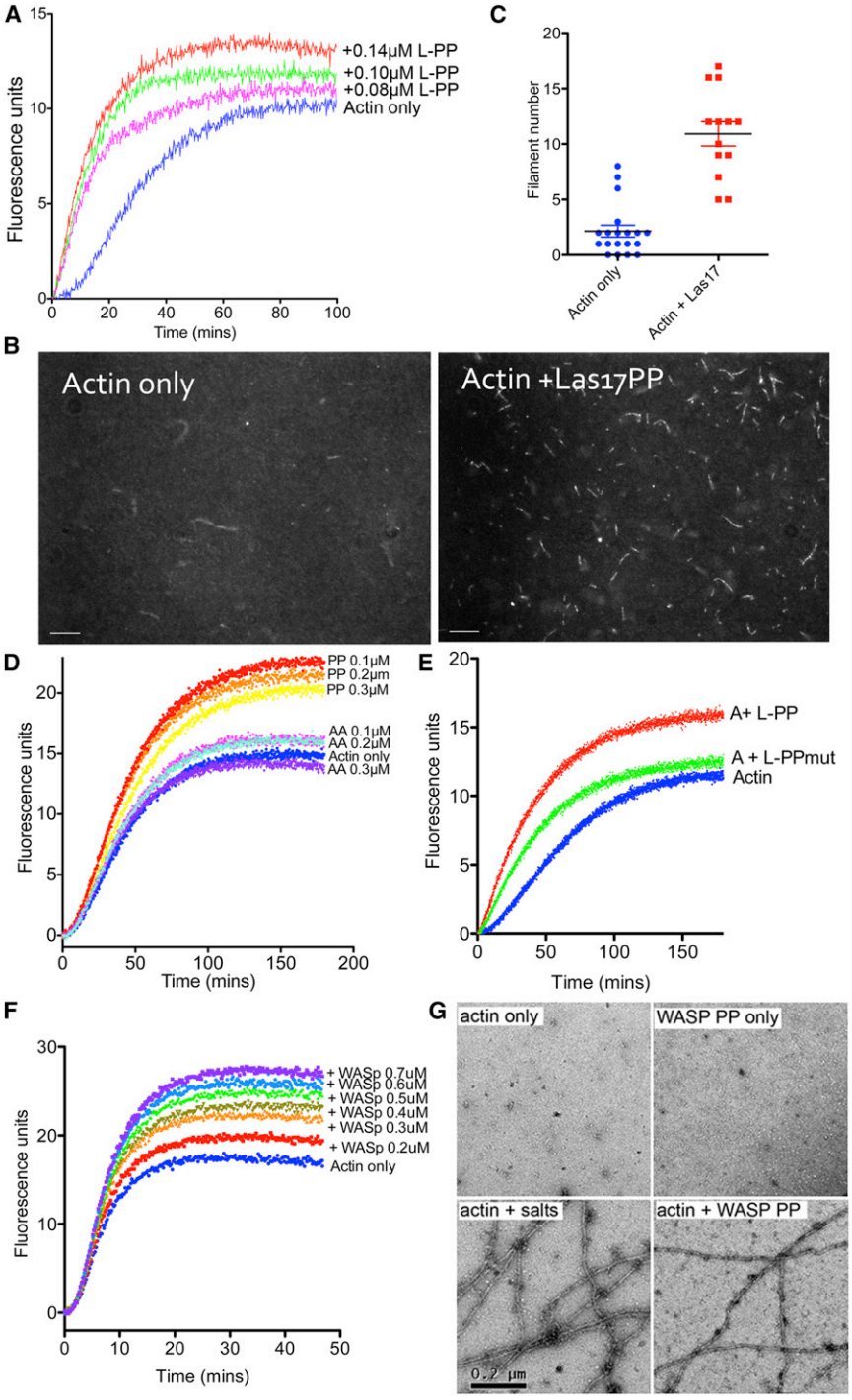

Figure 2. Las17PP Nucleates Actin Filaments

(A) Las17PP (L-PP) was cleaved from its GST tag and incubated at different concentrations (0.08 μM, 0.1 μM, and 0.14 μM) with 5 μM actin in the presence of 25 mM KCl, 1 mM $MgCl_2$, and 1 mM EGTA, in a pyrene-actin assay where actin polymerization can be followed from nucleation (lag phase) through to steady-state actin treadmilling.

(B) To determine whether Las17PP increases nucleation events, we incubated 3 μM actin (+ 0.4 μM Alexa 488 actin) with 0.14 μM Las17PP and visualized it after 30 min. Scale bar represents 5 μm.

(C) The number of actin filaments per unit area (1/20 of total image area) for up to 19 images was recorded and plotted graphically. The number of filaments in the two conditions is significantly different ($p \leq 0.0001$) by unpaired Student's t test. Mean ± SD is shown.

(D) Peptides corresponding to residues 501–528 were synthesized (PP), and a mutant peptide was also generated with PP-AA changes in positions 4 and 5 of each 5×PP tract (AA). Different concentrations of peptide were incubated with 5 μM actin in the presence of pyrene-actin and 25 mM KCl.

(E) A Las17PP mutant was generated (PP506,507AA; L-PPmut). Wild-type and mutant Las17PP (GST tag removed) were incubated at 0.14 μM with 3 μM actin in a pyrene-actin assay.

(F) WASP-PP was expressed and incubated with 5 μM actin at a range of concentrations from 0.2 to 0.7 μM in a pyrene-actin assay including 25 mM KCl.

(G) Actin filaments formed by WASP-PP were visualized by electron microscopy and are similar to those induced by salt. Scale bar represents 0.2 μm.

Las17PP and Las17-WH2 Are Both Required for Normal Growth and Actin Organization In Vivo

Analysis of cells expressing *act1-104* as the sole actin in cells revealed defects in endocytic patch movement, indicating the effect of inhibiting Las17PP binding (Figure S4). However, because this mutation may disrupt binding to other actin-binding proteins (e.g., formins Bni1 and Bnr1), we investigated Las17PP-actin function further through generation of Las17 mutations. Proline residues 506 and 507 have not been mapped as part of an SH3 interaction site; they gave the strongest defect in actin binding by two-hybrid analysis and were shown to contribute significantly to the extent of polymerization observed in vitro (Figures 1B and 2E). The effect of a complete Las17 WCA deletion domain has been studied [14], but the contribution of the actin-binding WH2 domain alone has not been analyzed. Thus, proline residues 506 and 507 were mutagenized to alanines to disrupt one site of PP-actin binding, and I555 was mutagenized to aspartate to disrupt actin binding through WH2 [27]. Mutant and wild-type *las17* were expressed under control of the Las17 promoter in cells. *las17* deletion causes cells to be temperature sensitive. This can be rescued by re-expression of *LAS17*. Increasingly defective growth was observed for I555D, PP506,507AA, the double mutation, and the null strain (Figure 4A). In wild-type cells with normally functioning actin, there were many polarized cortical patches of actin, whereas in *las17* deletion strains, there were few, bright cortical spots that were not polarized (Figure 4B). In the mutants, there was a loss in polarity of patches, though unlike in *las17* deletion mutants, patches appeared to become smaller and more numerous.

Uptake of the fluid phase dye Lucifer yellow is used to indicate defects in initial stages of endocytosis and also in later

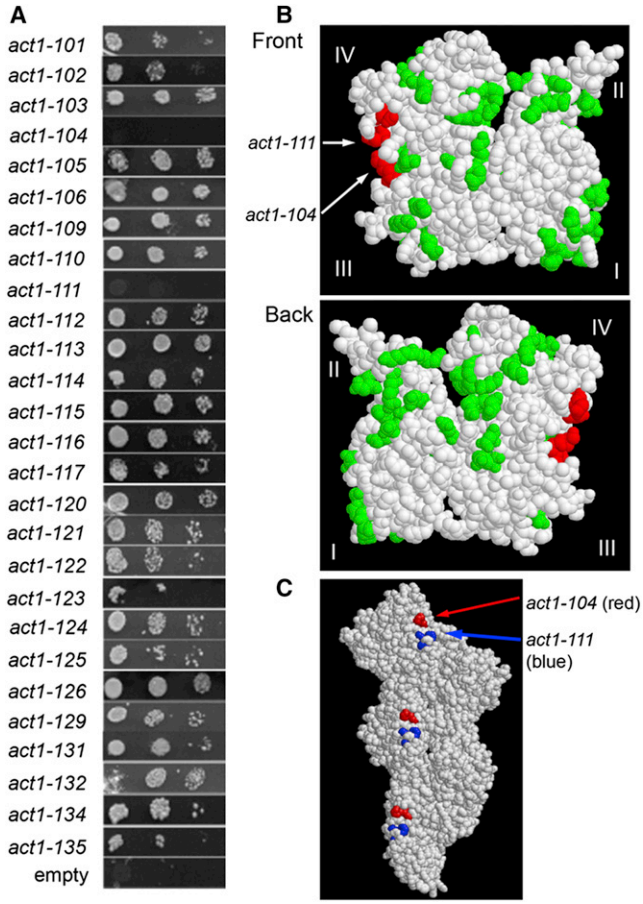

Figure 3. Las17PP Binds to Actin in a Region between Subdomains III and IV

(A) Yeast two-hybrid plasmids expressing 27 different actin alleles were tested for their ability to bind Las17PP. All except two of these actin alleles could interact with Las17PP. The noninteracting alleles were *act1-104* and *act1-111*.

(B) Structure of actin depicting the 27 alleles tested. Front and back views are shown. Interacting alleles are shown in green and noninteracting alleles in red.

(C) Filament model of actin depicting the *act1-104* mutated residues in red and *act1-111* residues in blue.

stages of trafficking to the vacuole. After incubation with cells expressing *LAS17*, dye uptake into large vacuolar structures is observed (Figure 4C). In *las17* deletion, there is greatly reduced dye uptake, though endosomal structures can be seen, indicating that some dye is endocytosed but then unable to undergo subsequent trafficking. In the single mutants, an increase in plasma membrane and endosomal staining is observed. Significantly, the double mutant has a phenotype highly reminiscent of the null strain, indicating that the two actin-binding sites together contribute the majority of Las17 function during endocytosis.

Mutations in Las17PP and Las17-WH2 Cause Different Defects in Endocytic Invagination

Live-cell imaging and analysis of single endocytic events has been highly informative about stages of endocytosis at which a protein functions [28, 29]. In order to determine whether distinct endocytic defects were caused by the proline or WH2 mutations, the behavior of an endocytic reporter, Sla1-mRFP, was analyzed in cells expressing wild-type or mutant *las17*. As shown in Figure 5A, patch tracking and kymographs from analysis of movies reveal differences in the effects of mutants. Whereas I555D appears to cause a defect during the invagination stage, the effect of the proline mutants appears to precede this stage, with a defect in the ability to stabilize the patch position. The double mutant shows no invaginations. Analysis of patch lifetime (Figure 5B) and patch intensity (Figure 5C) reiterates the importance of the PP residues in Las17 function. In particular, in the absence of functional WH2, Sla1-mRFP appears to be able to be recruited and stay at the site appropriately, though the time taken for invagination is prolonged. In contrast, in the PP506,507AA mutant, Sla1-mRFP takes a longer time to reach maximum recruitment at the site, indicating an earlier defect in endocytic patch function.

Discussion

Overall, our data demonstrate the presence of a novel actin-binding site in yeast Las17/WASP, within which proline residues play a central role in the binding interaction. Analysis of WASP-PP indicates that this region can also interact directly with actin, supporting the idea that PP domains may represent an evolutionarily conserved actin-binding site. The PP binding site on actin resides between subdomains III and IV of actin and is thus distinct from the WH2-domain actin-binding site. This study has focused on the PP-actin-binding interaction within the context of the yeast Las17 protein. Previous studies demonstrated that the Las17 WCA domain interacts with actin and Arp2/3 to promote nucleation and polymerization, and this was assumed to be the primary function of the protein. It was therefore unexpected when deletion of the WCA domain or just the Arp2/3-binding acidic domain gave only subtle phenotypes in vivo [13, 14], contrasting greatly with the slow-growing, temperature-sensitive, endocytically defective *las17* deletion strain [11] and suggesting that other regions of Las17 were critical to its function in vivo. Our data reveal a novel actin-binding region within PP tracts of Las17. When PP and WH2 mutations are combined, the cell phenotype is similar to the null, suggesting that the two sites contribute in an additive way to supply the major part of Las17 function. The severity of the PP mutation for growth, and the phenotype of the endocytic patch behavior, showing extensive lateral movement prior to invagination, suggests that the function of the PP site acts prior to that of the WCA domain. We propose a model outlined in Figure 6. Briefly, on arrival at the plasma membrane, the PP-rich region of Las17 is able to mediate multiple interactions with actin and thereby greatly increase the chances of nucleus formation by constraining movement of individual monomers. In this way, the region could act in a similar manner to the tandem WH2-domain nucleators [7, 27]. Actin filaments are generated, which from electron microscopy appear to be unbranched. These filaments then recruit Arp2/3 and possibly myosins to the endocytic site. Arp2/3, in conjunction with Las17, is then able to trigger a burst of actin polymerization to drive invagination of the membrane. However, the function of PP-driven actin nucleation does not appear to be simply generation of filaments for Arp2/3 recruitment. The actin formed at this stage appears to be critical for corralling the early proteins at the endocytic site, such that when PP sites are mutagenized, the endocytic site is observed to show erratic movement in the plane of the membrane. It is also possible that this actin corral serves as a platform against which to exert force during invagination against cell turgor [30].

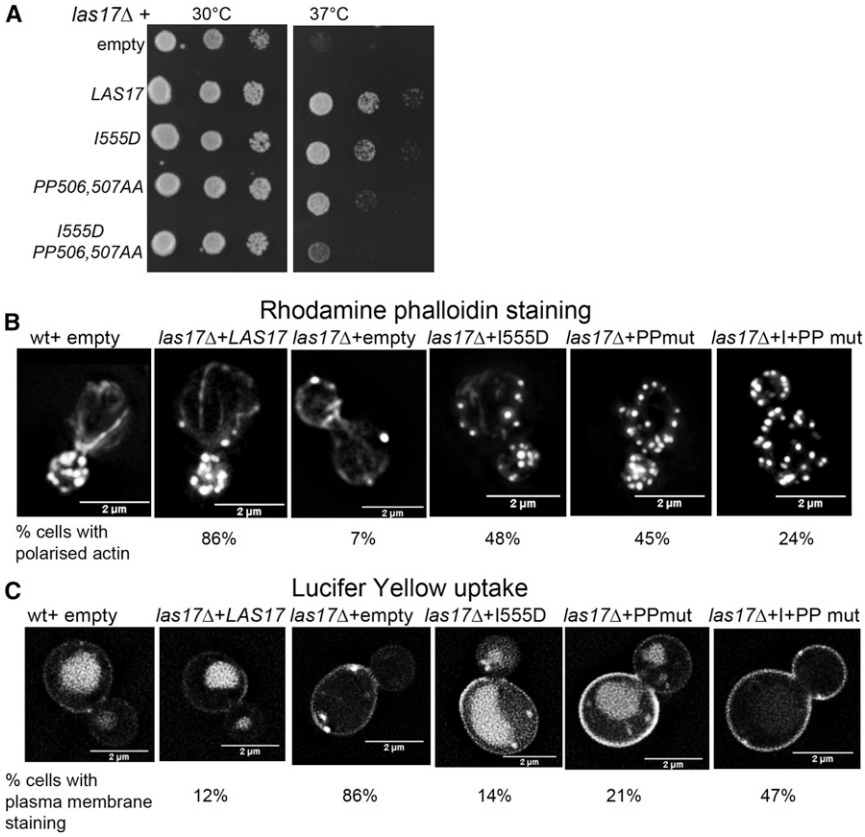

Figure 4. The Las17PP Mutant Has Defects in Growth, Actin Organization, and Endocytosis

Strains in which *las17* is deleted were transformed with plasmids carrying wild-type *LAS17*, *las17 I555D*, *las17 PP506,507AA*, *las17 I555D+ PP506,507AA*, or an empty plasmid. Expression levels of mutants were similar to wild-type (data not shown).

(A) Strains were spotted at 10-fold dilutions onto plates and incubated for 48 hr at 30°C or 37°C.

(B) Rhodamine-phalloidin staining was used to determine F-actin organization in cells at 30°C. The percentage of cells with polarized actin patches, defined as >75% patches in the bud, was quantified from three independent experiments ($n \geq 200$).

(C) Fluid-phase endocytosis was assessed by imaging Lucifer yellow uptake in cells expressing wild-type and mutant *las17*. The proportion of cells showing plasma membrane staining from three or more experiments ($n \geq 100$ cells) is shown below the images.

In previous reports, it has been shown that the proline-rich region of Las17 contributes positively to actin nucleation and polymerization [15, 31]. However, other in vitro experiments revealed that addition of the SH3-domain-containing proteins Sla1 and Bbc1 had an inhibitory effect, leading to a model in which Las17 is proposed to be recruited to the membrane and then held in an inhibited state until SH3 binding is released. This appears incompatible with our data in which Las17 PP function is required to generate actin filaments at an early stage of endocytosis, prior to invagination. However, in the previous experiments, the SH3 domains were added in excess of the concentration of Las17 [15, 31], which may allow binding of SH3 domains to a greater number of proline tracts, thus effectively outcompeting any actin-binding function of the PP domain. In both reported cases, there is a level of Arp2/3 and Las17 nucleation that does not appear to be inhibited by SH3-domain addition, and it is likely that this is the function attributable to the WCA domain. In vivo, the levels of Las17 are considered to be higher than those of these SH3-domain-containing proteins [32], making an inhibitory function less likely. Our data provide an alternative interpretation of the in vitro data and allow a simpler explanation for the function of the early Las17 recruitment to endocytic sites.

As well as identifying the PP domain as a new actin-binding region in Las17, we also demonstrated that the equivalent domain in WASP, the mammalian homolog of Las17, is able to interact with actin to promote polymerization. Although a nucleation activity was not observed in the pyrene-based assay, filaments could be generated in very low-salt conditions as shown by electron microscopy (Figure 1), suggesting the possibility that under appropriate conditions, the domain might nucleate filaments. Alternatively, the PP tracts could act to deliver actin monomers to actively growing filament ends.

This work opens many new avenues for research and also poses new questions. Foremost among these are the structural considerations for how PP tracts interact with actin and whether additional residues are involved in defining the affinity of the interaction. Furthermore, mutation of Las17 PP and WCA domains appears to cause distinct phenotypes, indicating sequential function. The nature of the proteins or modifications that regulate these actin-based functions is unknown, though it seems likely that this will be a possible role for some of the Las17 SH3-domain interactions. Finally, it is clear that proline tracts are found in many proteins. Although the nature of the minimal component for actin binding is not yet known, it is striking that 5 of the 8 proteins with two or more 5×PP are known actin nucleators, which is highly suggestive of the importance of the tract as we have described. Addressing the function of proline tracts not simply as profilin or SH3-binding sites but as independent actin-binding motifs in both characterized (e.g., Bni1) and uncharacterized proteins is likely to yield important new insights.

Experimental Procedures

Yeast Strains, Growth, and Plasmid Construction

Details of yeast strains, growth conditions, and plasmids are given in Supplemental Experimental Procedures. Transformations used lithium acetate [33]. For yeast two-hybrid assays, strains carrying binding-domain constructs and activation-domain constructs were crossed and diploids were selected on selective media. Diploids were grown overnight and assayed for β-galactosidase activity as described previously [33].

Protein Purification

Details of protein purification are given in Supplemental Experimental Procedures. Briefly, GST-expression plasmids were transformed into Lucigen OverExpress C41(DE3) cells. Protein was purified from 2 l of cells after induction by isopropyl β-D-1-thiogalactopyranoside (5 hr 37°C). Lysates were incubated with glutathione Sepharose beads (GE Healthcare) for 1 hr at 4°C and washed, and proteins were cleaved using PreScission Protease according to the manufacturer's instructions. Cleaved protein was buffer

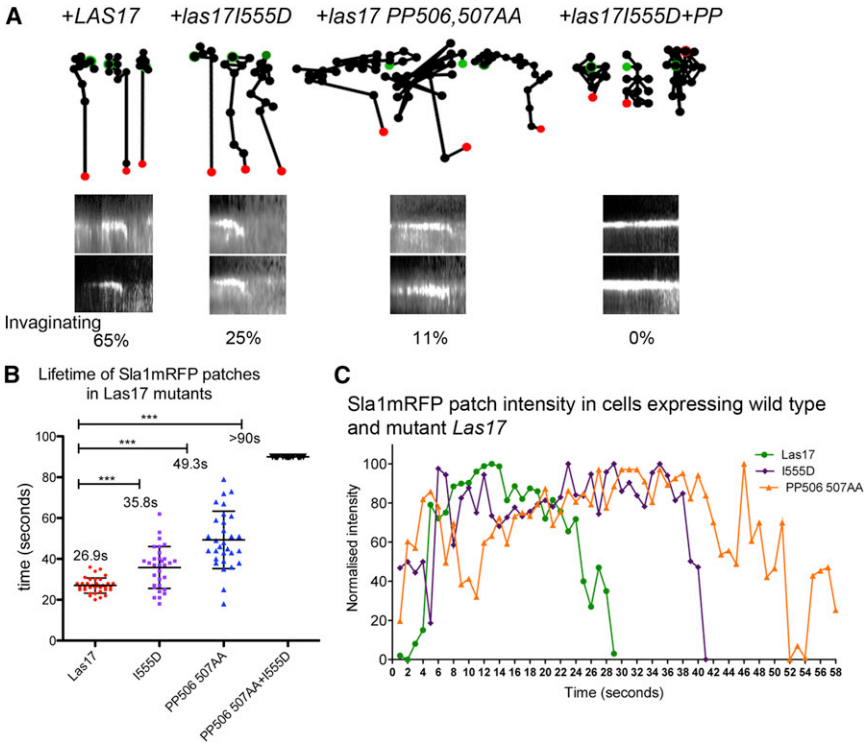

Figure 5. The Las17PP Mutant Has Defects in the Behavior of Single Endocytic Patches

Behavior of Sla1-mRFP-containing endocytic patches was analyzed from movies of wild-type or Las17 PP506,507AA mutant cells.

(A) Spot tracking was used to monitor movement of individual patches. Three representative tracks are shown for each strain. Green indicates assembly start point; red indicates disassembly point. Movement and behavior of the patches are also depicted in kymographs below the tracks. The percent of assembled patches that invaginate prior to disassembly was recorded ($n \geq 100$).

(B) Lifetime of Sla1-mRFP was measured in the presence of wild-type or mutant Las17. Error bars are SD of the mean lifetime. Significance of differences was analyzed by Student's t test; *** $p < 0.0001$.

(C) Fluorescence intensity was analyzed over the patch lifetime for Sla1-mRFP. Shown is the average of seven patches normalized to the wild-type maximum intensity value.

exchanged into G buffer (2 mM Tris-HCL [pH 8.0], 0.2 mM $CaCl_2$, 1 mM NaN_3, 0.5 mM dithiothreitol, 0.2 mM ATP), kept on ice at 4°C, and used within 24 hr. Rabbit skeletal muscle actin was purified and gel filtered as described previously [34]. Peptide was synthesized to >95% purity by Pi Proteomics (Huntsville, AL). See Supplemental Experimental Procedures for sequence.

Actin Assays

For G-actin-binding assays, glutathione beads with GST fusions were incubated with 5 μM G-actin + 10% fluorescent Alexa 568 actin in G buffer. Binding was assessed using fluorescence microscopy. High-speed pelleting assays were performed as described previously [34]. Briefly, 5 μM actin was incubated alone or with varying amounts of Las17 fragment as indicated. Polymerization salts, 10× KME (500 mM KCL, 10 mM $MgCl_2$, 10 mM EGTA, 100mM Tris-HCl [pH 8.0]), were added to 1×, and after 2 hr, samples were centrifuged at 350,000 × g. For fluorometry assays, 370 μl assays used 3–5 μM actin as indicated. Pyrene-actin was added to 5%, mixed thoroughly, and added to the fluorometry cuvette. Polymerization salts were mixed with Las17PP, WASP-PP, peptide, or G buffer to give final concentration of 0.5× KME before reading fluorescence. Polymerization was observed in a Cary Eclipse fluorometer (emission 364 nm, slit 10 nm round; excitation 385 nm, slit 20 nm).

Electron microscopy was performed using assays set up as for pelleting. Samples were adsorbed on carbon-coated copper grids and stained with 0.75% uranyl formate. Images were recorded on a Philips CM100 electron microscope using a Gatan MultiScan 794 CCD camera.

Fluorescence Microscopy

Fluorescence microscopy was performed on an Olympus IX81 inverted microscope, and data were deconvolved using AutoQuant software (Media Cybernetics). For live-cell imaging, cells were visualized after growing to early log phase. The distance of moving fluorescence spots was measured, and arbitrary profile of intensity values, image coordinates, and tracking of patch movements were established using ImageJ. Images were exported as TIFF files and assembled using Adobe Photoshop CS2. Kymographs were assembled using ImageJ. Statistical analysis of lifetimes was performed using GraphPad Prism software. Lucifer yellow uptake assays were performed as described previously [35] except that incubations were for 90 min. Rhodamine-phalloidin staining of actin structures was performed as described previously [36].

Supplemental Information

Supplemental Information includes four figures, two tables, and Supplemental Experimental Procedures and can be found with this article online at http://dx.doi.org/10.1016/j.cub.2012.12.024.

Acknowledgments

We would like to thank Steve Winder (University of Sheffield) for critical reading of the manuscript, David Amberg (Upstate University, Syracuse, NY) for sharing the Y2H actin allele collection, and Matt Welch (University of California, Berkeley) for the WASP-PWCA plasmid. This work was

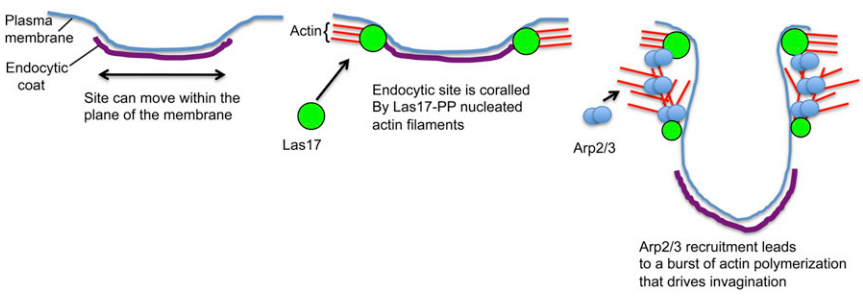

Figure 6. Proposed Model for Stages of Las17 Function

At early stages of endocytosis, coat proteins arrive at sites on the plasma membrane but their position is not highly restricted. Following recruitment of Las17 through interaction with one of its many binding partners, the PP region is active and able to nucleate formation of actin filaments that serve as a corral to stabilize the site. The filaments also serve to recruit Arp2/3, which can then interact with Las17 and type 1 myosins to promote an inward burst of actin polymerization required to drive membrane invagination.

supported by an MRC senior nonclinical fellowship to K.R.A. (G0601600). A.P.S. and A.N.U. were supported by studentships from the BBSRC.

Received: December 14, 2011
Revised: October 24, 2012
Accepted: December 13, 2012
Published: January 3, 2013

References

1. Winder, S.J., and Ayscough, K.R. (2005). Actin-binding proteins. J. Cell Sci. *118*, 651–654.
2. Campellone, K.G., and Welch, M.D. (2010). A nucleator arms race: cellular control of actin assembly. Nat. Rev. Mol. Cell Biol. *11*, 237–251.
3. Machesky, L.M., Atkinson, S.J., Ampe, C., Vandekerckhove, J., and Pollard, T.D. (1994). Purification of a cortical complex containing two unconventional actins from Acanthamoeba by affinity chromatography on profilin-agarose. J. Cell Biol. *127*, 107–115.
4. Sagot, I., Rodal, A.A., Moseley, J., Goode, B.L., and Pellman, D. (2002). An actin nucleation mechanism mediated by Bni1 and profilin. Nat. Cell Biol. *4*, 626–631.
5. Chesarone, M.A., and Goode, B.L. (2009). Actin nucleation and elongation factors: mechanisms and interplay. Curr. Opin. Cell Biol. *21*, 28–37.
6. Rodal, A.A., Sokolova, O., Robins, D.B., Daugherty, K.M., Hippenmeyer, S., Riezman, H., Grigorieff, N., and Goode, B.L. (2005). Conformational changes in the Arp2/3 complex leading to actin nucleation. Nat. Struct. Mol. Biol. *12*, 26–31.
7. Qualmann, B., and Kessels, M.M. (2009). New players in actin polymerization—WH2-domain-containing actin nucleators. Trends Cell Biol. *19*, 276–285.
8. Ahuja, R., Pinyol, R., Reichenbach, N., Custer, L., Klingensmith, J., Kessels, M.M., and Qualmann, B. (2007). Cordon-bleu is an actin nucleation factor and controls neuronal morphology. Cell *131*, 337–350.
9. Chereau, D., Boczkowska, M., Skwarek-Maruszewska, A., Fujiwara, I., Hayes, D.B., Rebowski, G., Lappalainen, P., Pollard, T.D., and Dominguez, R. (2008). Leiomodin is an actin filament nucleator in muscle cells. Science *320*, 239–243.
10. Quinlan, M.E., Heuser, J.E., Kerkhoff, E., and Mullins, R.D. (2005). Drosophila Spire is an actin nucleation factor. Nature *433*, 382–388.
11. Li, R. (1997). Bee1, a yeast protein with homology to Wiscott-Aldrich syndrome protein, is critical for the assembly of cortical actin cytoskeleton. J. Cell Biol. *136*, 649–658.
12. Winter, D., Lechler, T., and Li, R. (1999). Activation of the yeast Arp2/3 complex by Bee1p, a WASP-family protein. Curr. Biol. *9*, 501–504.
13. Galletta, B.J., Chuang, D.Y., and Cooper, J.A. (2008). Distinct roles for Arp2/3 regulators in actin assembly and endocytosis. PLoS Biol. *6*, e1.
14. Sun, Y.D., Martin, A.C., and Drubin, D.G. (2006). Endocytic internalization in budding yeast requires coordinated actin nucleation and myosin motor activity. Dev. Cell *11*, 33–46.
15. Rodal, A.A., Manning, A.L., Goode, B.L., and Drubin, D.G. (2003). Negative regulation of yeast WASp by two SH3 domain-containing proteins. Curr. Biol. *13*, 1000–1008.
16. Yarar, D., D'Alessio, J.A., Jeng, R.L., and Welch, M.D. (2002). Motility determinants in WASP family proteins. Mol. Biol. Cell *13*, 4045–4059.
17. Amberg, D.C., Basart, E., and Botstein, D. (1995). Defining protein interactions with yeast actin in vivo. Nat. Struct. Biol. *2*, 28–35.
18. Tonikian, R., Xin, X., Toret, C.P., Gfeller, D., Landgraf, C., Panni, S., Paoluzi, S., Castagnoli, L., Currell, B., Seshagiri, S., et al. (2009). Bayesian modeling of the yeast SH3 domain interactome predicts spatiotemporal dynamics of endocytosis proteins. PLoS Biol. *7*, e1000218.
19. Holt, M.R., and Koffer, A. (2001). Cell motility: proline-rich proteins promote protrusions. Trends Cell Biol. *11*, 38–46.
20. Tanaka, M., and Shibata, H. (1985). Poly(L-proline)-binding proteins from chick embryos are a profilin and a profilactin. Eur. J. Biochem. *151*, 291–297.
21. Thanabalu, T., Rajmohan, R., Meng, L., Ren, G., Vajjhala, P.R., and Munn, A.L. (2007). Verprolin function in endocytosis and actin organization. Roles of the Las17p (yeast WASP)-binding domain and a novel C-terminal actin-binding domain. FEBS J. *274*, 4103–4125.
22. Higgs, H.N., Blanchoin, L., and Pollard, T.D. (1999). Influence of the C terminus of Wiskott-Aldrich syndrome protein (WASp) and the Arp2/3 complex on actin polymerization. Biochemistry *38*, 15212–15222.
23. Burston, H.E., Maldonado-Báez, L., Davey, M., Montpetit, B., Schluter, C., Wendland, B., and Conibear, E. (2009). Regulators of yeast endocytosis identified by systematic quantitative analysis. J. Cell Biol. *185*, 1097–1110.
24. Matsuo, R., Kubota, H., Obata, T., Kito, K., Ota, K., Kitazono, T., Ibayashi, S., Sasaki, T., Iida, M., and Ito, T. (2005). The yeast eIF4E-associated protein Eap1p attenuates GCN4 translation upon TOR-inactivation. FEBS Lett. *579*, 2433–2438.
25. Chereau, D., Kerff, F., Graceffa, P., Grabarek, Z., Langsetmo, K., and Dominguez, R. (2005). Actin-bound structures of Wiskott-Aldrich syndrome protein (WASP)-homology domain 2 and the implications for filament assembly. Proc. Natl. Acad. Sci. USA *102*, 16644–16649.
26. Schutt, C.E., Myslik, J.C., Rozycki, M.D., Goonesekere, N.C.W., and Lindberg, U. (1993). The structure of crystalline profilin-beta-actin. Nature *365*, 810–816.
27. Aguda, A.H., Xue, B., Irobi, E., Préat, T., and Robinson, R.C. (2006). The structural basis of actin interaction with multiple WH2/beta-thymosin motif-containing proteins. Structure *14*, 469–476.
28. Kaksonen, M., Toret, C.P., and Drubin, D.G. (2005). A modular design for the clathrin- and actin-mediated endocytosis machinery. Cell *123*, 305–320.
29. Robertson, A.S., Smythe, E., and Ayscough, K.R. (2009). Functions of actin in endocytosis. Cell. Mol. Life Sci. *66*, 2049–2065.
30. Aghamohammadzadeh, S., and Ayscough, K.R. (2009). Differential requirements for actin during yeast and mammalian endocytosis. Nat. Cell Biol. *11*, 1039–1042.
31. Feliciano, D., and Di Pietro, S.M. (2012). SLAC, a complex between Sla1 and Las17, regulates actin polymerization during clathrin-mediated endocytosis. Mol. Biol. Cell *23*, 4256–4272.
32. Ghaemmaghami, S., Huh, W.K., Bower, K., Howson, R.W., Belle, A., Dephoure, N., O'Shea, E.K., and Weissman, J.S. (2003). Global analysis of protein expression in yeast. Nature *425*, 737–741.
33. Kaiser, C., Michaelis, S., and Mitchell, A. (1994). Methods in Yeast Genetics: A Laboratory Course Manual (Cold Spring Harbor, NY: Cold Spring Harbor Laboratory Press).
34. Winder, S.J., Hemmings, L., Maciver, S.K., Bolton, S.J., Tinsley, J.M., Davies, K.E., Critchley, D.R., and Kendrick-Jones, J. (1995). Utrophin actin binding domain: analysis of actin binding and cellular targeting. J. Cell Sci. *108*, 63–71.
35. Dulic, V., Egerton, M., Elguindi, I., Raths, S., Singer, B., and Riezman, H. (1991). Yeast endocytosis assays. Methods Enzymol. *194*, 697–710.
36. Hagan, I.M., and Ayscough, K.R. (2000). Fluorescence Microscopy in Yeast. In Protein Localization by Fluorescence Microscopy: A Practical Approach, V.J. Allan, ed. (Oxford: Oxford University Press), pp. 179–205.